Journal of Ceramic Processing Research. Vol. 12, No. 5, pp. 602~605 (2011)

JOURNAL OF
Ceramic
Processing Research

Preparation and sintering behavior of Al_2O_3-Y_2O_3/ZrB_2 composite powders

Jie-Guang Song* and Fang Wang

Jiujiang Key Laboratory of Green Remanufacturing, School of Mechanical and Materials Engineering, Jiujiang University, Jiujiang 332005, China

Zirconium diboride (ZrB_2) has some excellent physical properties and chemical stability, it has been widely applied in many fields, but the sintering densification of ZrB_2 is very difficult, and it is easily oxidized at high temperature. In order to improve the disadvantages of ZrB_2, Al_2O_3-Y_2O_3/ZrB_2 composite powders were prepared by a co-precipitation methods. When the pH is 9, the encapsulted structure of $A1(OH)_3$-$Y(OH)_3$/ZrB_2 composite powders is best. Through analyzing ZrB_2 surface status with SEM, EDS, TEM and XRD, the $A1_2O_3$-Y_2O_3/ZrB_2 composite powders were prepared by calcining at 600 °C in argon. The density of ZrB_2-YAG ceramics with Al_2O_3-Y_2O_3 composite powders added is higer than that of ZrB_2-YAG ceramics, which indicates the $A1_2O_3$-Y_2O_3/ZrB_2 composite powders are more easily prepared than high density ZrB_2-YAG ceramics.

Key wards: ZrB_2, YAG, Composite powders, co-precipitation methods, Sintering behavior.

Introduction

Zirconium diboride (ZrB_2) has attracted substantial interest because of its attractive chemical and physical properties, such as a high melting point, superior hardness, and low electrical resistance. ZrB_2 has several applications such as Hall-Heroult cell cathodes for the electrochemical processing of aluminum, evaporation boats, crucibles for handling molten metals, thermowall tubes for steel refining, thermocouple sleeves for high-temperature uses, nozzles, plasma electrodes, or as dispersoids in metal and ceramic-matrix composites for heaters and igniters [1-4]. However, ZrB_2 is easily oxidized in high-temperature air, which impacts on its high-temperature strength and restricts its range of applications [5-6]. Some excellent oxidation resistance materials are considered as an assistant phase for ZrB_2 to prepare ZrB_2 composite materials to improve the high-temperature performance of ZrB_2 materials, such as Al_2O_3-ZrB_2, SiC-ZrB_2, LaB_2-ZrB_2, and ZrO_2-ZrB_2 [7-9].

Yttrium aluminum garnet (YAG or $Y_3Al_5O_{12}$) adopts a cubic garnet structure and is of great interest as a high-temperature engineering material due to its high temperature strength coupled with low creep rate, which indicates that YAG ought to be a suitable matrix or reinforcing material [10-13].

To make ZrB_2 ceramics achieve a high density and better oxidation resistance, Al_2O_3-Y_2O_3/ZrB_2 composite powders were prepared, and the sintering behavior of Al_2O_3-Y_2O_3/ZrB_2 composite powders is investigated in this paper.

*Corresponding author:
Tel : +86-792-8313632
Fax: +86-792-8311239
E-mail: songjieguang@163.com

Materials and Experiments

Analytical grades aluminum nitrate, yttrium nitrate, and ammonia were used. Commercially-available submicrometer ZrB_2 powder (99.5% purity and 10 μm mean particle diameter) was used for the preparation of a powder mixture by a co-precipitation method. The submicrometer ZrB_2 powder was first dispersed in deionized water. The suspension was stirred for 30 minutes, and then the composite solution of $A1(NO_3)_3$ and $Y(NO_3)_3$ (Al : Y = 5 : 3) was added slowly. The suspensions were further stirred to break up possible agglomerates. Then ammonia (NH_4OH) was added in to the suspension at various titration rates to certain final pH values. Then the suspension was stirred further for 1 hour, filtered, the precipites washed four times (three times with deionized water and once with absolute ethyl alcohol) and dried at 100 °C to obtain ZrB_2 ceramic composite powder. The composite powder was calcined at 600 °C in argon. Then the composite raw materials were encased in a graphite mould, sintered, demoulded and tested.

The shell of the composite particles was analyzed by scanning electron microscopy (SEM; Model : JSM-5610LV, Wuhan, Japan) and transmission electron microscopy (TEM; Model : JEM-2010, Wuhan, Japan). Elemental identification of ZrB_2 particle surfaces was performed by an energy dispersive X-ray spectrometer (EDS; Model : JCXA-733, Wuhan, Japan). Phase analysis was performed at different conditions by an X-ray powder diffractometer (XRD; Model : D/Max-RB, Wuhan, Japan). The microstructure of the ceramics was studied by scanning electron microscopy (SEM; Model : JSM-5610LV, Wuhan, Japan).

Results and Discussion

Influence of pH on the microstructure of $Al(OH)_3$-$Y(OH)_3$/ZrB_2 composite powders

$Al(OH)_3$-$Y(OH)_3$/ZrB_2 composite powders was synthesized at particular value of the pH. The configuration of an original and coated ZrB_2 surface is compared in Fig. 1. A smooth surface is presented on the original ZrB_2 particles. The ZrB_2 surface is coated with a few floccules of $Al(OH)_3$ precipitate at pH = 7. Because the pH satisfies the production of the $Al(OH)_3$ precipitates from the $Al(NO_3)_3$ solution via heterogeneous nucleation, the Al^{3+} does not form $Al(OH)_3$ precipitates completely. However, a layer of symmetrical floccules with $Al(OH)_3$ and $Y(OH)_3$ precipitates is coated on the ZrB_2 surface at pH = 9, which is about 150 nm thick. The thickness of the coating layer is decreased at pH = 11. Many small spheroidal masses remain with the $Y(OH)_3$ precipitates on the ZrB_2 surfaces. With an increase in the pH of the ZrB_2 suspension, the entire process from $Al(NO_3)_3$ and $Y(NO_3)_3$ solution to $Al(OH)_3$ and $Y(OH)_3$ precipitate is shown in four steps: no deposit, heterogeneous nucleation, homogeneous nucleation, and a complete deposit [14]. The relationship of the Al^{3+} complex and pH is shown in Fig. 2. After the complete deposition process, $Al(OH)_3$ is formed as an AlO^2 soluble complex in the suspension of ZrB_2 by a continuous increase of the pH [15]. However, $Y(OH)_3$ precipitates do not dissolve in the alkaline solution, which still exist on the ZrB_2 surface. When the pH is 9, $Al(OH)_3$-$Y(OH)_3$/ZrB_2 composite powders with a better coating quality are formed.

Charactorization of Al_2O_3-Y_2O_3/ZrB_2 composite powders

Phase analysis of ZrB_2 particles is shown in Fig. 3, which indicates the main phase is the ZrB_2 phase, but a different phase is found as the conditions are changed. The backgrounds of Fig. 3(b) and (c) are higher than for Fig. 3(a). Because ZrB_2 particles are coated with amorphous $A1(OH)_3$ and $Y(OH)_3$ precipitate, Fig. 3(c) shows the Al_2O_3 and Y_2O_3 phases, because $A1(OH)_3$ and $Y(OH)_3$ were dehydrated.

Elemental identification and the shell configuration of ZrB_2 particle surfaces under different conditions are shown in Fig. 4. The original ZrB_2 particles only show Zr and B, but the surface of coated ZrB_2 particles shows Al and Y in addition to Zr and B. $A1(NO_3)_3$ and $Y(NO_3)_3$ have formed $A1(OH)_3$ and $Y(OH)_3$ precipitates at pH = 9 coated on the surface of ZrB_2 particles through the co-precipitation. The surface of the original ZrB_2 particles is very smooth (Fig. 4(a)). Coated ZrB_2 particles (dried at 100 °C) are shown in Fig. 4(b); the surface of ZrB_2 particles is coated with a layer of floccules of $A1(OH)_3$ and $Y(OH)_3$ precipitates. Coated ZrB_2 particles (calcined at 600 °C) are shown in Fig. 4(c); the surfaces of ZrB_2 particles are not smooth and many fine particles are evident. Fig. 3(c) is the phase analysis of composite particles calcined at 600 °C, and the background of the phase picture is high, which means the composite particles contain $A1(OH)_3$ and $Y(OH)_3$.

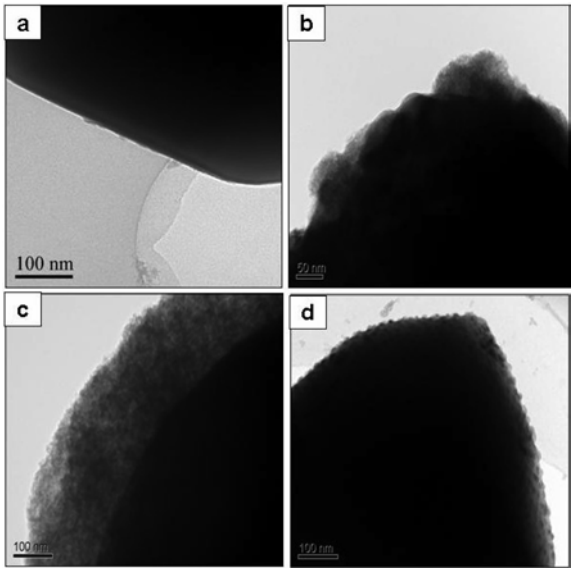

Fig. 1. Topographic characteristics of $A1(OH)_3$-$Y(OH)_3$/ZrB_2 composite powders under different pH conditions (a-Original, b-pH = 7, c- pH = 9 and d- pH = 11).

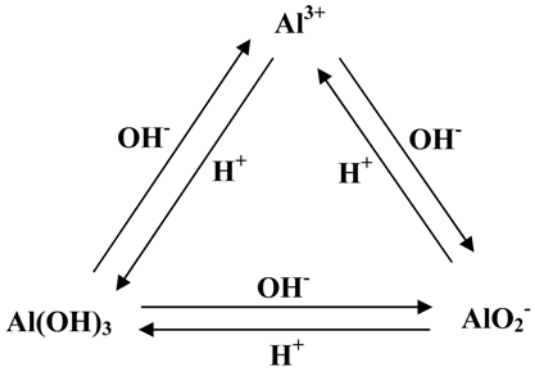

Fig. 2. Relation of Al compounds and pH.

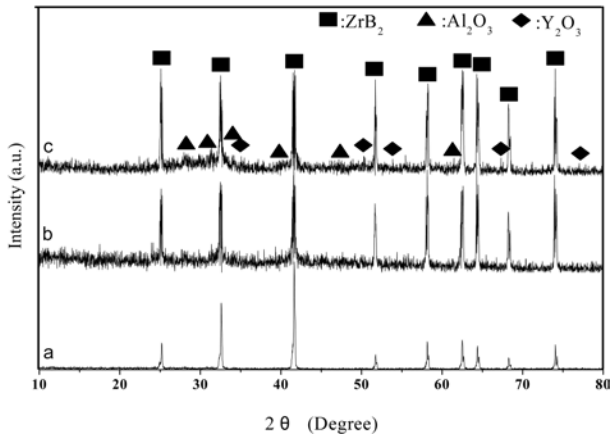

Fig. 3. XRD of ZrB_2 after treating under different conditons (a-Original ZrB_2, b-Coated ZrB_2 with $A1(OH)_3$-$Y(OH)_3$ and c-Coated ZrB_2 with Al_2O_3-Y_2O_3).

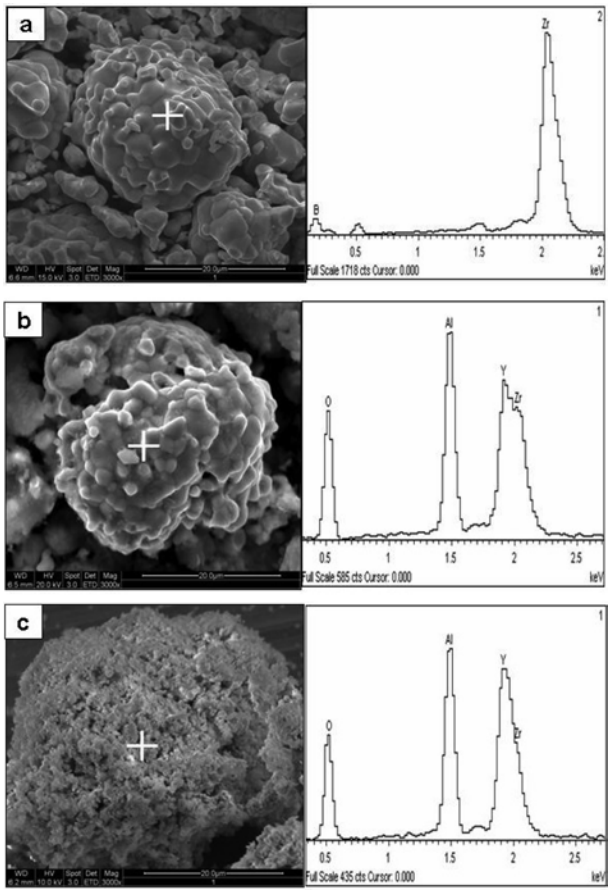

Fig. 4. SEM and EDS of ZrB_2 after treating under different conditons (a-Original ZrB_2, b-Coated ZrB_2 with $A1(OH)_3$-$Y(OH)_3$ and c-Coated ZrB_2 with Al_2O_3-Y_2O_3).

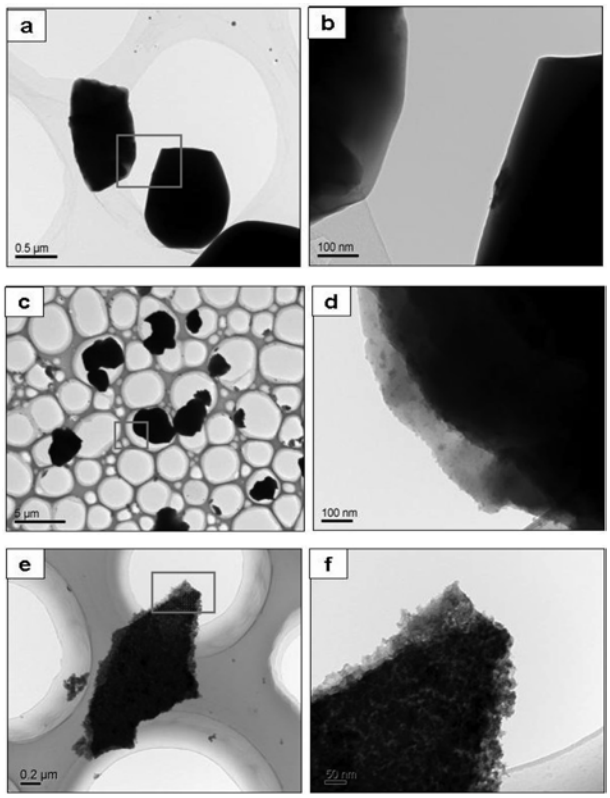

Fig. 5. TEM of ZrB_2 after treating under different conditons (a and b-Original ZrB_2, c and d- Coated ZrB_2 with $A1(OH)_3$-$Y(OH)_3$, e and f- Coated ZrB_2 with Al_2O_3-Y_2O_3 after being calcined at 600ºC).

TEM of ZrB_2 particles under different conditions are shown in Fig. 5. The surface of the original ZrB_2 particles is very smooth (Figs. 5(a) and (b)). TEM of coated ZrB_2 particles (dried at 100 ºC) is shown in Figs. 5(c) and (d), the surface of ZrB_2 particles is coated with a layer of floccule fine pricipitates about 30 nm in size, which is uniform and compact. TEM of coated ZrB_2 particles (calcined at 600 ºC) is shown in Figs. 5(e) and (f); the surface of ZrB_2 particles is coated with Al_2O_3-Y_2O_3 nanoparticles to form $A1_2O_3$-Y_2O_3/ZrB_2 composite powders; the Al_2O_3-Y_2O_3 shell is about 30 nm thick, which is uniform. $A1_2O_3$-Y_2O_3/ZrB_2 composite powders were successfully synthesized as shown by their characterization.

Sintering behavior of Al_2O_3-Y_2O_3/ZrB_2 composite powders

The sintering curve for preparing ZrB_2-20 wt%YAG multiphase ceramic materials from different composite raw materials with the spark plasma sintering techniqe is shown in Fig. 6. The spark plasma sintering Z-axis displacement shows the shrinkage state of a ceramic body during the sintering process, when the value of the Z-axis displacement increases, this indicates the ceramic body is shrinking. The Z-axis displacement shows the shrinkage

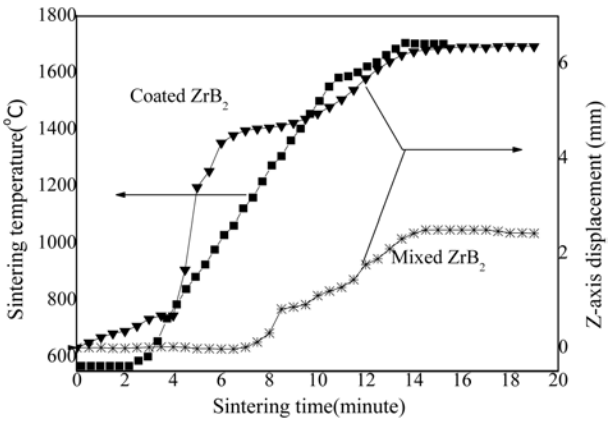

Fig. 6. Sintering shrinkage curve of ZrB_2-20 wt%YAG ceramics.

state of adding Al_2O_3-Y_2O_3 composite powders and YAG powders, respectively. The composite powders with Al_2O_3-Y_2O_3 added show a rapid shrinkage displacement from 700 ºC to 950 ºC, where the biggish shrinkage displacement also is shown from 950 ºC to 1600 ºC, the Z-axis displacement is not varied basically above 1600 ºC. The sintering temperature curve is broken down into four parts, which include a preheating process below 700 ºC, a reaction process from 700 ºC to 950 ºC, a sintering process from 950 ºC to 1600 ºC, and an adjustment of the microstructure above 1600 ºC. The densification occurs mainly during the reaction process and sintering process,

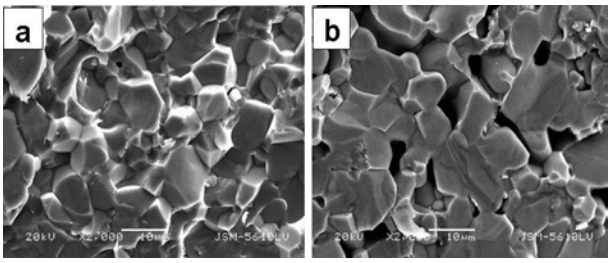

Fig. 7. SEM of ZrB_2-20 wt%YAG ceramics (a-Coated ZrB_2 with Al_2O_3-Y_2O_3, b-Mixed ZrB_2 with YAG).

that is, sintering from 700 °C to 1600 °C. YAG is produced from 700 °C to 950 °C. The reaction temperature is lower than the 1100 °C for synthesizing YAG powders from Al_2O_3-Y_2O_3 composite powders, because ZrB_2 particles are changed electrically during the entire sintering process, which produces a plasma among ZrB_2 particles to purify the nearby particle surfaces and increase the sintering activity [16-18].

However, the Z-axis displacement for powders with YAG added shows a lower shrinkage displacement below 950 °C; a larger shrinkage displacement is shown from 950 °C to 1600 °C, the Z-axis displacement is not varied basically above 1700 °C. The Z-axis displacement adding the different powders both show the same shrinkage state from 950 °C to 1600 °C, YAG melts above 950 °C, the temperature is lowered because of the action of the plasma. Because the results of the two routes both show the Z-axis displacement is not varied basically above 1700 °C, a sintering temperature of 1700 °C is choosen for preparing high density ZrB_2-YAG multiphase ceramics, the microstructure of ZrB_2-YAG multiphase ceramics are shown in Fig. 7, which indicates the density of ZrB_2-YAG ceramics with Al_2O_3-Y_2O_3 composite powder added is higer than that of ZrB_2-YAG ceramics with YAG powder added.

Conclusions

Al_2O_3-Y_2O_3/ZrB_2 composite powders were prepared by a co-precipitation methods. When the pH is 9, the encapsulted structure of $A1(OH)_3$-$Y(OH)_3$/ZrB_2 composite powders is the best. By analyzing the ZrB_2 surface status with SEM, EDS, TEM and XRD, the $A1_2O_3$-Y_2O_3/ZrB_2 composite powders were prepared under the calcining conditions of 600 °C in argon. The density of ZrB_2-YAG ceramics with Al_2O_3-Y_2O_3 composite powder added is higer than that of ZrB_2-YAG ceramics with YAG powder added, which indicates the $A1_2O_3$-Y_2O_3/ZrB_2 composite powders are more easily prepared and have a higher density than ZrB_2-YAG ceramics.

Acknowledgments

The authors are thankful for the financial support provide by the Science and Technology Support Fund for Young Scholars of the Educational Department of Jiangxi Province, China (Grant No.GJJ09595), and for the apparatus provided by The Center for Materials Testing and The Functionally Gradient Material (FGM) Research Laboratory of Wuhan University of Technology, China.

References

1. L. Silvestroni, D. Sciti, C. Melandri and S. Guicciardi, J. Eur. Ceram. Soc. 30 (2010) 2155-2164.
2. S.M. Zhu, W.G. Fahrenholtz, G.E. Hilmas and S.C. Zhang, Mater. Sci. Eng. A 459 (2007) 167-17.
3. J.G. Song, G.C. Ji and S.B. Li, J. Ceram. Process. Res. 10 (2009) 428-432.
4. P. Hu, X.H. Zhang and J.C. Han, J. Am. Ceram. Soc., 93 (2010) 345-349.
5. I.B. Bankovskaya, M.P. Semov and A.E. Lapshin, Glass Phys. Chem., 31 (2005) 433-438.
6. A.L. Chamberlain, W.G. Fahrenholtz and G.E. Hilmas, J. Am. Ceram. Soc., 89 (2006) 450-456.
7. J.G. Song, D.M. Du and Y.Y. Ju, J. Ceram. Process. Res., 11 (2010) 494-497.
8. A. Bellosi, F. Monteverde and D. Sciti, Int. J. Appl. Ceram. Tec., 3 (2006) 32-40.
9. H.F. Hu, Q.K. Wang and Z.H. Chen, Ceram. Int., 36 (2010) 1011-1016.
10. X.X. Li and W.J. Wang, Powder Technol., 196 (2009) 26-29.
11. S.J. Wang, Y.B. Xua, P.X. Lua, C.F. Xu and W. Cao, Mater. Sci. Eng. B, 127 (2006) 203-206.
12. Y.M. Zhang and H.M. Yu, Ceram. Int., 35 (2009) 2077-2081.
[13] J. G. Song, Mater. Manuf. Process., 25 (2010) 724-729.
14. R. Vallepu, A.M. Jimenez, T. Terai and A. Mikuni, J. Ceram. Soc. Jap., 114 (2006) 624-629.
15. A.V. Radha and P.V. Kamath, Bull. Mater. Scie., 26 (2003) 661-666.
16. N. Frage, S. Kalabukhov and N. Sverdlov, J. Eur. Ceram. Soc., 30 (2010) 3331-3337.
17. J.G. Song, D.M. Du and Y.Y. Ju, J. Reinf. Plast. Comp., 29 (2010) 710-717.
18. Y.H. Sang, H. Liu and Y.H. Lv, J. Alloy. Compd., 490 (2010) 459-462.